

# Estimation of the Gain and Threshold of the Stretch Reflex with a Novel Subspace Identification Algorithm

Kian Jaleleddini and Robert E. Kearney

**Abstract**— Reflex stiffness is often modeled as a Hammerstein system comprising a cascade of a static nonlinear element and a linear dynamic element. The nonlinearity is frequently modeled as a half wave rectifier so that changes in the reflex response can only be modeled by changes in the parameters of the linear element. This is an oversimplification since there are physiological mechanisms that could change both the threshold of the nonlinearity and the linear dynamics. This study explores the ability of a new subspace identification algorithm to distinguish changes in parameters of the nonlinear element from those of the linear element. Simulation studies demonstrate that the method does so very effectively even in the presence of substantial output noise. Pilot experiments in which the method was applied to stretch reflex EMG data revealed that both the threshold of the nonlinearity and the gain of the linear element change with muscle activation.

## I. INTRODUCTION

Joint stiffness defines the dynamic relation between the position of the joint and the torque acting about it [1]. Studying joint stiffness is of great importance due to its applications in many fields. Consequently, identification of its dynamic behavior has been extensively investigated in the past years in many joints [1], [2], [3].

Joint stiffness consists of two components. The first is the intrinsic component which is due to mechanical properties of the limb, joint, tissue and active muscles. The second is the reflex component which originates from the stretch reflex arc [1]. Some years ago our laboratory demonstrated that ankle joint stiffness could be described well by the model shown in Fig. 1 [4]. In this model, the total joint torque is the sum of the outputs of intrinsic and reflex pathways. The reflex path is modeled as a nonlinear-linear (NL) cascade system (a Hammerstein structure) which relates the joint velocity to the reflex torque. The nonlinearity resembles a half wave rectifier. The linear component of the reflex path is a second- or third-order system with a delay of about 40 ms [5].

The nonlinearity in the reflex path reflects the unidirectional velocity sensitivity of the stretch reflex. Previous studies showed that the nonlinearity in the reflex path of the ankle joint resembles a half wave rectifier [6], [5]. In other words, there is a reflex response when the extensor muscle is stretched but no response when it is shortened. Other studies such as [2], [3] assumed a more complex shape for the nonlinearity in elbow joint reflex stiffness.

K. Jaleleddini and R. E. Kearney are with the Department of Biomedical Engineering, McGill University, 3775 University, Montréal, Québec H3A 2B4, Canada. [seyed.jaleleddini@mail.mcgill.ca](mailto:seyed.jaleleddini@mail.mcgill.ca), [kearney@mcgill.ca](mailto:kearney@mcgill.ca).

This work has been supported by CIHR.

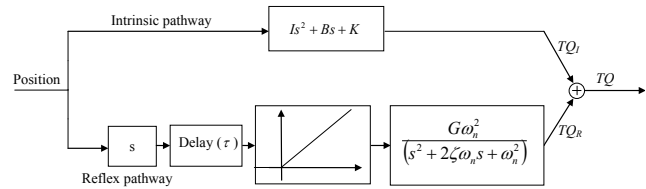


Fig. 1. Parallel-cascade model of ankle joint stiffness.

Our laboratory showed that the reflex response at the ankle changes with joint position and/or level of muscle activation [5]. The nonlinearity was assumed to be a half-wave rectifier, so all changes in the reflex response were attributed to the linear system parameters, i.e., gain ( $G$ ), damping parameter ( $\zeta$ ) and natural frequency ( $\omega_n$ ). However, it is also possible that the shape of the nonlinear element might change with joint position and/or level of muscle activation, e.g., changes in the threshold. Thus, physiological mechanism such as the motoneuron pool excitability and static fusimotor activity could change the reflex threshold. Conversely, presynaptic inhibition, changes in interneuronal activity, and dynamic fusimotor activity might modulate the gain of the reflex path [7], [8]. Consequently, it is important to be able to distinguish between these two types of changes.

In this work, we apply a recently developed Hammerstein identification algorithm [9] and evaluate its performance in distinguishing between the estimation of the threshold of the nonlinearity from the gain of the linear component. Subsequently, we apply the new algorithm to experimental data and study the behavior of the reflex EMG as a function of muscle activation level.

This paper is organized as follows: Section II provides the problem formulation of a Hammerstein system and discusses the advantages of the new identification algorithm. Section III provides the result of simulation using a model of stretch reflex. Section IV presents the experimental results and Section V provides some concluding remarks.

## II. PROBLEM FORMULATION AND IDENTIFICATION ALGORITHM

A *single-input-single-output* SISO Hammerstein system consists of a zero memory static nonlinearity followed by a linear system as illustrated in Fig. 2 [10]. The nonlinearity can be approximated by a basis function expansion (power polynomial, Tchebyshev, Hermite, etc) as:

$$w(k) = f(u(k)) \simeq \sum_{i=1}^n \alpha_i g_i(u(k)) \quad (1)$$

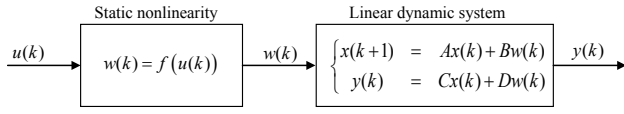


Fig. 2. Hammerstein system model.

where,  $g_i(\cdot)$  is the  $i^{\text{th}}$  basis function and  $\alpha_i$  is its corresponding coefficient. Then, as shown in [11], the total Hammerstein model can be formulated as a MISO state space model:

$$\begin{cases} x(k+1) = Ax(k) + B_\alpha U(k) \\ y(k) = Cx(k) + D_\alpha U(k) + n(k) \end{cases} \quad (2)$$

where,  $U(k)$  is a vector of inputs constructed by a basis function expansion as  $[g_1(u(k)), \dots, g_n(u(k))]^T$  where  $g_i(\cdot)$  is the element of the expansion.  $n(k)$  is the additive noise,  $x(k)$  is the state vector,  $A$ ,  $C$  are the matrices of the linear part and  $B_\alpha$  and  $D_\alpha$  are:

$$B_\alpha = \begin{bmatrix} b_1\alpha_1 & \dots & b_1\alpha_n \\ \vdots & \ddots & \vdots \\ b_m\alpha_1 & \dots & b_m\alpha_n \end{bmatrix} \quad (3)$$

$$D_\alpha = [d\alpha_1 \quad \dots \quad d\alpha_n] \quad (4)$$

where  $\{b_1, \dots, b_m\}$  and  $\{d\}$  are the parameters of the linear state space matrices, i.e.,  $B$  and  $D$ . Note that each element of these matrices is related to the parameters of both the linear and nonlinear elements.

This formulation transforms a SISO Hammerstein model to a MISO linear system whose state space matrices can be estimated using the method described in [11]. In particular, at the first step, it estimates the matrices  $A$  and  $C$  using a subspace approach. Then, it estimates the elements of  $B_\alpha$  and  $D_\alpha$  using a least square approach. However, each element of  $B_\alpha$  and  $D_\alpha$  is related to the parameters of both the nonlinear component and the linear part. Therefore, while the resulting model predicts the output well, it provides no insight into the elements of interest. This is important because in biomedical applications, it is often of interest to understand the underlying system rather than simply to construct a model that can predict the output well [9].

We recently developed an algorithm that estimates the parameters of the nonlinearity ( $\alpha_i$ ,  $i \in 1, \dots, n$ ) from those of the linear part, i.e., ( $b_j$  and  $d$ ,  $j \in 1, \dots, m$ ). This approach formulates the problem using the minimum number of parameters required in the state space model in a nonlinear optimization framework. It then solves the optimization problem using an iterative least square approach. Since it uses the minimum number of parameters and the global convergence of the nonlinear optimization problem is guaranteed, we expect it to be very robust in the presence of large output noise [9].

### III. SIMULATION ANALYSIS

#### A. Input Signal

The frequency and amplitude structures of the input signal play an important role in system identification. Due to

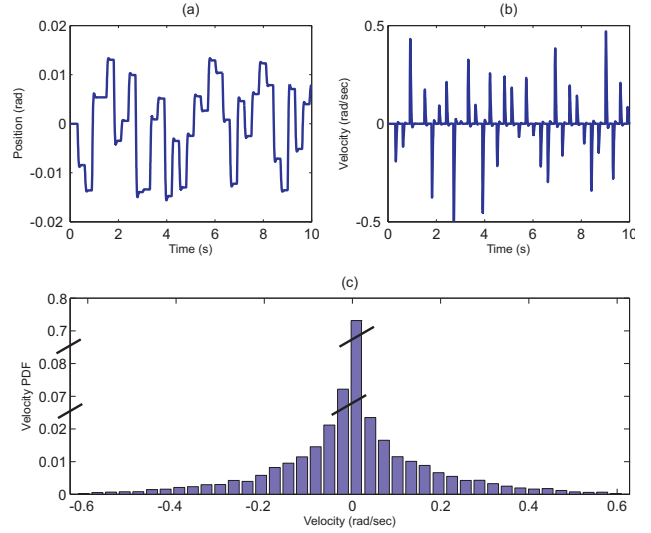


Fig. 3. Input signal used for simulation: (a) A realization of the position; (b) A realization of the velocity; (c) Probability distribution of the velocity.

the presence of nonlinearities in the joint stiffness system, the amplitude structure of the input velocity is particularly important, since the mean absolute velocity must be low to preserve the stretch reflex [1], [12].

A position input signal used frequently in the identification of joint stiffness is a stochastic binary signal (PRBS) with small amplitude around a desired operating point. The histogram of its velocity shows only three distinct levels corresponding to zero, positive, and negative velocities [13]. While this type of input excites the linear system well, its amplitude structure is not rich enough to estimate the static nonlinearity properly. With three input levels an infinite number of polynomials can be fit between these three levels. To address this, we used a position input comprising samples from a uniform distribution at 300 ms as shown in Fig. 3. The probability distribution of the resulting velocity has a much richer set of values which should result in more effective estimation of the shape of the static nonlinearity.

#### B. Method

The performance of the algorithm was evaluated using simulation of the small signal model of stretch reflex stiffness of the human ankle shown in Fig. 4. The nonlinearity comprised a threshold  $t_1$  described by:

$$f(u(k)) = \frac{(u(k) - t_1) + (u(k) - t_1)\text{sgn}(u(k) - t_1)}{2} \quad (5)$$

where  $\text{sgn}$  is the sign function. The continuous-time transfer function of the linear element was:

$$H(s) = \frac{e^{-t_d s} G_r \omega_n^2}{s^2 + 2s\zeta\omega_n + \omega_n^2} \quad (6)$$

where  $s$  is the Laplace variable,  $G_r$  is the linear system's gain,  $\zeta$  is the damping parameter and  $\omega_n$  is the natural frequency of the second order system. There is also a delay of  $t_d$  seconds.

The parameters of the Hammerstein system were:  $G_r = 25$ ,  $\zeta = 0.98$ ,  $\omega_n = 20$ ,  $t_d = 0.04$  and  $t_1 = 0$  values similar

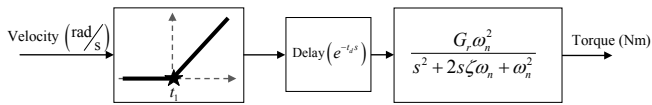


Fig. 4. Hammerstein model of reflex stiffness.

to those derived previously from experimental data [5]. The model was simulated in MATLAB Simulink at 1 KHz for sixty seconds. The simulated input and output signals were decimated to 100 Hz. Realizations of Gaussian, white noise were added to the output to simulate experimental noise; the amplitude of the noise was adjusted to generate the required *signal to noise ratio* (SNR).

The performance of the new algorithm was compared to that of two other well-known algorithms for Hammerstein system identification-*Hunter-Korenberg* H-K [10] and *separable least squares* SLS algorithms [13].

### C. Results

Fig. 5 shows the models estimated by the three methods obtained with a SNR of 5 db. The nonlinearities estimated by subspace and SLS algorithms closely resembled the theoretical half wave rectifier (Fig. 5(a)). Similarly, the *impulse response functions* (IRF) estimate for the linear component of the model estimated using subspace and SLS were very similar to that used in the simulation, Fig. 5(b). In contrast, the nonlinearity estimated using H-K was not similar to the simulated half-wave rectifier and the estimated IRF was different. The similarity of the predicted reflex torque to the noise free output was quantified in terms of the *variance accounted for* (VAF). We found VAF of 99.8%, 99.6%, 79.2% for subspace algorithm, SLS and H-K respectively. These simulation results demonstrate that H-K gives biased results in the presence of large output noise.

Next, we compared the efficiency of the algorithms in estimating the linear component. To do so,  $t_1$  was set to zero and the linear system gain was varied from 10 to 40 and SNR was fixed at 5 db. We then used Monte-Carlo simulation with 100 trials at each gain. We compared the estimated IRF to the simulated one in terms of VAF between the estimated and simulated IRFs for the three algorithms. Fig. 6 shows the mean value of the VAF bracketed by its standard deviation. The subspace algorithm performed the best. It had the highest VAFs and the lowest variance, indicated by the error bars.

Another set of Monte Carlo simulations were carried out to assess the ability of the algorithm to distinguish between changes in gain and threshold. The linear system gain  $G_r$  and nonlinearity threshold  $t_1$  were varied systematically and 100 trials were simulated at each threshold/gain combination. We modeled the estimated static nonlinearity by the parametric equation (5). Fig. 7(a) presents the mean value of the predicted gain. Fig. 7(b) shows the random error associated with each operating point i.e., the standard deviation of the error in the parameter estimate. Fig. 7(c) and (d) shows the results for the identification of the threshold. It is apparent that the gain and threshold were estimated reliably and independently

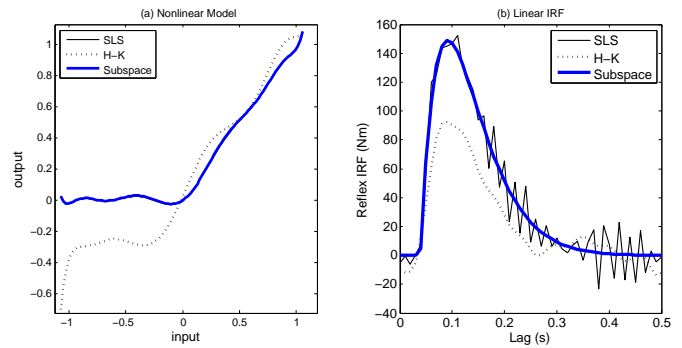


Fig. 5. Identified models of stretch reflex from simulation data.

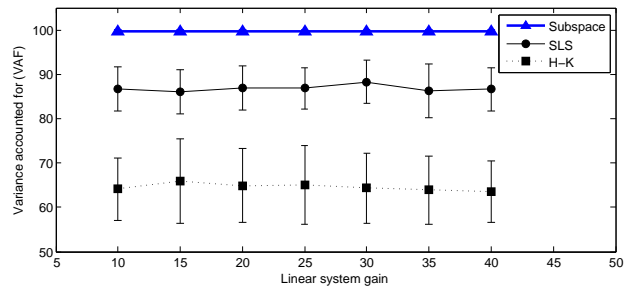


Fig. 6. The accuracy of the estimated linear model IRFs.

To quantify these results we fitted planes to the data shown in Fig. 7 and to corresponding results for the SLS and HK methods. Ideally these should have a slope of 1 for the gain and threshold (Fig. 7 (a), (c)). The results are summarized in table I. The subspace and SLS methods accurately separated the gain and threshold (i.e. slopes were close to 1), while the H-K method was quite biased. The SSE using the subspace algorithm was smaller than that for SLS demonstrating that the random error associated with the estimation was smaller using subspace.

## IV. EXPERIMENTS

### A. Method

To evaluate the performance of the algorithm under practical conditions we used it to estimate the dynamic relation between ankle velocity and reflex EMG in the triceps surae. This relation has been modeled previously as a Hammerstein system involving a unidirectional, rate sensitive nonlinearity.

The experimental methods were similar to those described in [4], [5], [13] except that the input signal was that used

TABLE I  
ESTIMATION OF GAIN AND THRESHOLD

		SLS	H-K	Subspace
Gain	Slope	1.031	0.5339	1.024
	SSE	2184	8474	1525
	R-square	0.9951	0.9365	0.9966
Threshold	Slope	1.03	0.6297	1.059
	SSE	0.5078	1.7380	0.2288
	R-square	0.9846	0.8748	0.9934

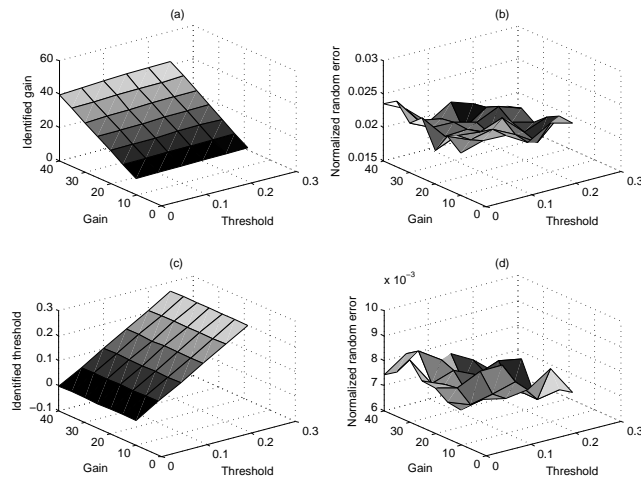


Fig. 7. Estimation accuracy of the Hammerstein model; (a) mean value of the predicted gains; (b) random error associated with the estimation of gain; (c) mean value of the predicted thresholds; (d) random error associated with the estimation of threshold.

in Section III. Two subjects were recruited and gave informed consent to the experimental procedures, which had been reviewed and approved by McGill University Research Ethics Board. Lateral and medial Gastrocnemius EMGs were recorded using surface electrodes. The mean angle of the ankle joint was set to neutral position (90 degrees). Ankle torque was low-pass filtered in real time and provided to the subject as visual feedback signal; the subject was asked to maintain a constant torque. Data were recorded for sixty seconds at sampling frequency of 1000 Hz and then decimated to 100 Hz for analysis.

The subjects were then asked to maintain three torque levels 5% MVC<sub>D</sub>, 0% MVC<sub>D</sub>, 5% MVC<sub>P</sub>, where MVC is the *maximum voluntary contraction* torque recorded in the plantar or dorsiflexion directions.

### B. Result

Fig. 8 shows the Hammerstein system estimated between the velocity and EMG for a typical subject with the new algorithm. It is evident that during plantarflexing contractions, when TS muscle was active, i.e., 5% of MVC<sub>P</sub>, the threshold was close to 0 and the amplitude of the IRF was large. This is consistent with previous findings [5]. However, when the muscle was at rest, the threshold increased significantly as evidenced by the shift in the nonlinearity to the right while the amplitude of IRF dropped to around 2. During dorsiflexing contraction, i.e., 5% of MVC<sub>D</sub>, the amplitude of the IRF decreased further while the threshold was located between the two previous cases.

## V. CONCLUSIONS

We showed that the new algorithm can successfully separate and estimate changes in the threshold of the nonlinearity from changes in the gain of the linear subsystem. In comparison with other algorithms it is more robust in the presence of output noise and provides more accurate results.

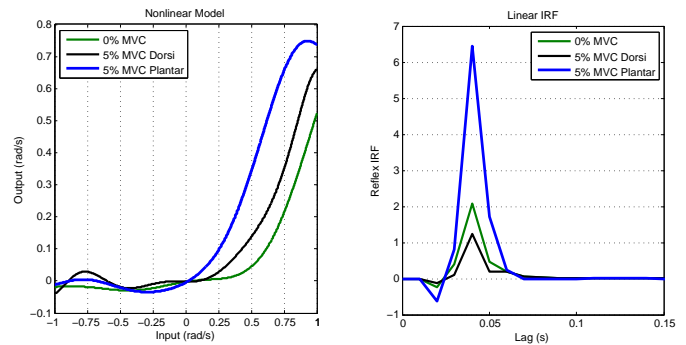


Fig. 8. Hammerstein models estimated from reflex EMG at different torque levels.

In practice, it is not possible to measure reflex torque independently since the torque recorded is the summation of voluntary, reflex and intrinsic components. Consequently, we used EMG as the output since it is an indicator of muscle activity but not related to the intrinsic response. Hence, the performance of the algorithm was evaluated using the EMG from triceps surae (TS). The results showed that the threshold remains close to zero while the TS muscle is active and is positive otherwise. The gain was higher when TS was active than while the muscle was at rest or TA was active.

## REFERENCES

- [1] R. E. Kearney and I. W. Hunter, "System identification of human joint dynamics," *Crit Rev Biomed Eng*, vol. 18, pp. 55–87, 1990.
- [2] E. J. Perreault, P. E. Crago, and R. F. Kirsch, "Estimation of intrinsic and reflex contributions to muscle dynamics," *IEEE Trans Biomed Eng*, vol. 47, pp. 1413–1421, 2000.
- [3] L. Q. Zhang and W. Z. Rymer, "Simultaneous and nonlinear identification of mechanical and reflex properties of human elbow joint muscles," *IEEE Trans Biomed Eng*, vol. 44, no. 12, 1997.
- [4] R. E. Kearney, R. B. Stein, and L. Parameswaran, "Identification of intrinsic and reflex contributions to human ankle stiffness dynamics," *IEEE Trans Biomed Eng*, vol. 44, no. 6, pp. 493–504, 1997.
- [5] M. M. Mirbagheri, H. Barbeau, and R. E. Kearney, "Intrinsic and reflex contributions to human ankle stiffness: variation with activation level and position," *Exp Brain Res*, vol. 135, no. 4, pp. 423–436, 2000.
- [6] R. E. Kearney and I. W. Hunter, "System identification of human triceps surae stretch reflex dynamics," *Exp Brain Res*, vol. 51, pp. 117–127, 1983.
- [7] P. Matthews, "The differentiation of two types of fusimotor fibre by their effects on the dynamic response of muscle spindle primary endings," *Experimental Physiology*, vol. 47.
- [8] —, "Muscle spindles and their motor control," *Physiological Reviews*, pp. 219–288, 1964.
- [9] K. Jaleleddini and R. E. Kearney, "An identification algorithm for hammerstein systems using subspace method," in *Proceedings of IFAC (to appear)*, 2011.
- [10] I. W. Hunter and M. J. Korenberg, "The identification of nonlinear biological systems: Wiener and Hammerstein cascade models," *Biol Cybern*, vol. 55, no. 2-3, pp. 135–144, 1986.
- [11] M. Verhaegen and D. Westwick, "Identifying MIMO Hammerstein systems in the context of subspace model identification methods," *International Journal of Control*, vol. 63, no. 2, pp. 331–349, 1996.
- [12] R. B. Stein and R. E. Kearney, "Nonlinear behavior of muscle reflexes at the human ankle joint," *J. Neurophysiol*, vol. 73, no. 1, pp. 65–72, 1995.
- [13] D. Westwick and R. Kearney, "Separable least squares identification of nonlinear Hammerstein models: Application to stretch reflex dynamics," *Ann Biomed Eng*, vol. 29, pp. 707–718, 2001.